4.9 SUPERROTATION IN AN AXISYMMETRIC SHALLOW WATER MODEL OF THE UPPER TROPOSPHERE

Karen M. Shell*[1] and Isaac Held[2]

[1]Scripps Institution of Oceanography, University of California, San Diego, CA

[2]Geophysical Fluid Dynamics Laboratory, Princeton, NJ

1. INTRODUCTION

Superrotation refers to zonally averaged zonal winds that have a greater angular momentum than anywhere on the surface of the earth. In order for the circulation to be inertially stable, the angular momentum of the zonal winds must decrease poleward; thus equatorial winds have the highest angular momentum. In addition, the earth's greatest angular momentum is at the equator. Thus, the atmosphere is superrotating if and only if the winds at the equator are westerly.

On the earth, the equatorial tropospheric winds are slightly easterly, so they have less angular momentum than the earth's surface at the equator. Thus, the earth's troposphere is not superrotating. However, superrotation occurs during the westerly phase of the Quasi-Biennial Oscillation (QBO) in the stratosphere, as well as on other planets, such as Jupiter and Saturn, and on our sun. These cases raise the question of whether the earth's troposphere could be superrotating under earth-like conditions.

Superrotation has appeared in simple models of the earth's atmosphere. Suarez and Duffy (1992) obtained superrotating states in a two-layer model when they applied a zonally asymmetric tropical heating. For certain strengths of the forcing, they found multiple equilibria in equatorial wind strength. Once superrotation was established in the model, the system would remain superrotating even if they removed the asymmetric heating. Saravanan (1990) used a two-layer model as well but applied a torque rather than asymmetric heating to produce superrotation. Recently, Huang et al (2001) found slight superrotation in a coupled GCM climate change simulation with tripled $C0_2$. These experiments suggests the possibility that tropospheric superrotation could occur on the earth, though much more work is needed to determine if these model results are realistic. Held summarizes the research on superrotation in earth-like atmospheric models (2001).

Suarez and Duffy and Saravanan attributed the bifurcations they obtained to a feedback between the forcing (whether generated by asymmetric heating or an applied torque) and the eddies. The forcing accelerates equatorial winds, and the eddies tend to decelerate equatorial winds. However, the effectiveness of the eddies decreases as the wind speed increases. Thus, increasing the forcing leads to stronger equatorial winds and thus less deceleration by the eddies, resulting in a positive feedback.

We looked for a similar bifurcation in an axisymmetric shallow water model of the upper troposphere. The model includes a torque that is directly applied to the equatorial region. In addition, the transport of mass (and thus momentum) from a non-moving lower layer can decelerate the flow around the equator. This deceleration depends on the wind speed at the equator, which depends on the strength of the forcing. We are interested in whether this feedback allows multiple equilibria for some ranges of the forcing. Since the equatorial zonal wind is always westerly when forcing is applied to this model, we looked for multiple steady superrotating states, one weakly superrotating and one strongly superrotating, for the same set of parameters.

2. THE MODEL

We modeled the troposphere using an axisymmetric (no variation in the longitudinal direction) one-and-a-half layer isentropic model on a sphere. The lower layer does not move, but it can exchange mass with the upper layer, thus affecting the height and zonal velocity of the upper layer. The upper portion of the troposphere is modeled using the shallow water equations for a spherical isentropic layer. The model determines the zonal velocity, u, meridional velocity, v, and height of the upper layer, h, as a function of time, t, and latitude, ϕ:

$$\frac{\partial u}{\partial t} + \frac{v}{a}\frac{\partial u}{\partial \phi} - 2\Omega v \sin\phi - \frac{uv\tan\phi}{a} = F + R - ku \quad (1)$$

$$\frac{\partial v}{\partial t} + \frac{v}{a}\frac{\partial v}{\partial \phi} + 2\Omega u \sin\phi + \frac{u^2\tan\phi}{a} = -\frac{g^*}{a}\frac{\partial h}{\partial \phi} - kv \quad (2)$$

$$\frac{\partial h}{\partial t} + \frac{1}{a\cos\phi}\frac{\partial hv\cos\phi}{\partial \phi} = -\frac{h - h_{eq}}{\tau}, \quad (3)$$

where F is an applied forcing. The system is relaxed to a radiative equilibrium height, $h_{eq}(\phi)$, and

$$R = \begin{cases} \frac{h-h_{eq}}{\tau}\frac{u}{h} & (h - h_{eq} < 0) \\ 0 & (h - h_{eq} > 0) \end{cases} \quad (4)$$

is the deceleration of the zonal momentum due to mass moving from the lower layer to the upper layer as part of this height relaxation. Ω is the rotation rate, a is the radius of the earth, k is the frictional parameter, g^* is the reduced gravity, and τ is the relaxation time. All values are in MKS units.

* *Corresponding author address:* Karen M. Shell, Univ. of California, 9500 Gilman Dr, Mail code 0224, La Jolla, CA 92093-0224; e-mail: kshell@ucsd.edu.

The forcing F for the system is an applied torque centered around the equator and constant in time, and it represents a flux of momentum from the lower layer:

$$F = F_0 \cos^n \phi,$$

where F_0 is the forcing at the equator.

The height of the upper layer is relaxed back to the "radiative equilibrium" height, h_{eq}, which simulates the effects of radiation on the system. When radiation warms a portion of air in the lower layer, its potential temperature increases, and it moves to the upper layer, increasing the height of the upper layer. When the upper layer cools, some air moves down into the lower layer, decreasing the height of the upper layer. The radiative equilibrium height decreases away from the equator and then goes to a constant near the pole:

$$h_{eq} = \begin{cases} h_{0eq} - \frac{a\Omega u_{0eq}}{g^*} \sin^2 \phi & (|\phi| < \phi_c) \\ h_{0eq} - \frac{a\Omega u_{0eq}}{g^*} \sin^2 \phi_c & (|\phi| > \phi_c) \end{cases} \quad (5)$$

where h_{0eq} is the radiative equilibrium height at the equator and u_{0eq} is the corresponding geostrophic wind at the equator.

The relaxation back to the equilibrium height also affects the zonal momentum budget through term R in equation (1). Air that is brought up from the lower layer carries with it the momentum from the lower layer. Since the momentum of the lower layer is less that that of the upper layer, this process decreases the zonal momentum in the upper layer. However, air that moves from the upper layer down to the lower layer carries with it the momentum of the upper layer and thus does not affect the momentum in the upper layer. Presumably surface friction returns the velocity in the lower layer to zero. Note that the relaxation mass flux also should affect the meridional velocity. However, we have omitted this effect from equation (2) because v is very close to geostrophic balance.

Term R is the key term in our model, because it provides the positive feedback to the forcing. At the equator, the forcing must balance the height relaxation term and friction. Since friction increases as the forcing (and thus the wind speed) increases, the height relaxation term is the required term for a bifurcation in this system.

Figure 1 shows the steady state of the model with no forcing. For this run, we used values of $a = 6.37 \times 10^6$ m, $\Omega = 7.292 \times 10^{-5}$ rad/s, $g^* = 9.81 \times 0.1$ ms^{-2}, $\tau = 900000$ s, $k = 5 \times 10^{-9}$ s^{-1}, $h_{0eq} = 20000$ m, $u_{0eq} = 60$ m/s, and $\alpha = 0.5$. The number of grid points is 300. These are the default values for all runs.

While the model uses similar parameters to those of the earth, it is not entirely earth-like. The atmosphere is not well-represented as two isentropic layers. The difference in potential temperature between the equator and the poles is about the same as the difference between the surface and the tropopause. Thus, the real atmosphere does not have an isentrope which divides the troposphere into an upper and lower layer.

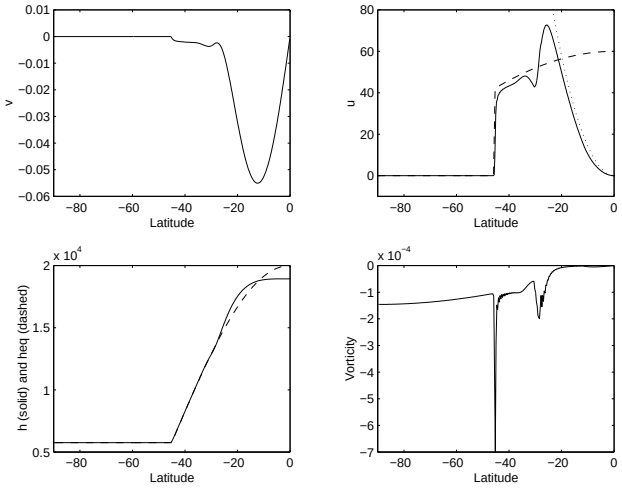

Figure 1: Steady state of the model with no forcing. The solid line is the computational model result. The dotted line is u from momentum conservation, and the dashed line is the radiative equilibrium result.

3. ANALYTICAL CALCULATIONS

In order to study the system more closely, we used a simple analytical model which approximates the full system of equations. The analytical model seeks to describe the state of the system using only u and h at the equator. By requiring that u and h are in steady state at the equator, we can determine which of these states is an equilibrium solution for a given set of parameters. This information gives us an idea of where to look for multiple equilibria in the full model.

The relation of the circulation to u and h at the equator can be explored using a simple Hadley cell model similar to the one used in Held and Hou (1980). The domain is divided into two regions. Close to the equator, the solution for h conserves angular momentum while towards the poles, the solution is just the "radiative equilibrium" solution, h_{eq}. By matching these two solutions, we can determine the critical latitude, ϕ_c, which separates them.

Equation (5) describes the radiative equilibrium solution. To determine the angular momentum conserving solution, h_m, assume the height is in geostrophic balance with the angular momentum conserving wind:

$$u_m = \frac{u_0 + \Omega a \sin^2 \phi}{\cos \phi}, \quad (6)$$

where u_0 is the zonal velocity at the equator. Integrating the geostrophic terms in equation (2) using the small angle approximation and the fact that $u_0 << \Omega a$,

$$h_m = h_0 - \frac{2a\Omega}{g^*} \left[u_0 \frac{\phi^2}{2} + \Omega a \frac{\phi^4}{4} \right], \quad (7)$$

where h_0 is the height of the layer at the equator.

Imposing continuity of h at ϕ_c and mass conservation and assuming $u_0 << \Omega a$, $h_{0eq} \approx h_0$, and ϕ_c small yields equations for the critical latitude and the height at the equator in terms of u_0:

$$\phi_c^2 = \frac{5}{3}\frac{u_{0eq} - u_0}{\Omega a}$$

$$h_0 - h_{0eq} = -\frac{5}{18g^*}(u_{0eq} - u_0)^2. \quad (8)$$

Note that to get a real value for ϕ_c, u_0 must be less than u_{0eq}.

In order for u_0 and h_0 to be in steady state, the applied torque at the equator must balance the friction and the momentum exchange due to relaxation of the height to equilibrium:

$$F = \frac{h_{0eq} - h_0}{\tau}\frac{u_0}{h_0} + ku_0 \quad (h_0 < h_{0eq}). \quad (9)$$

Assuming the system is not far from radiative equilibrium, we approximate the height in the denominator as a constant, h_{0eq}. Nondimensionalizing by

$$h_0 = Hh_{0eq},\ u_0 = Uu_{0eq},$$

equations (8) and (9) become:

$$1 - H = p(U-1)^2 \quad (10)$$

$$1 - H = \frac{q}{U} - r \quad (11)$$

where

$$q = \frac{F\tau}{u_{0eq}},\ p = \frac{5}{18}\frac{u_{0eq}^2}{g^* h_{0eq}},\ r = k\tau,$$

with q, p, and r all positive.

We are looking for solutions of these two equations for which $U < 1$ and $0 < H < 1$, since our analytical model requires that $u_0 < u_{0eq}$ and $0 < h_0 < h_{0eq}$. Equilibrium solutions are solutions of the cubic equation

$$U^3 - 2U^2 + U\left(1 + \frac{r}{p}\right) - \frac{q}{p} = 0. \quad (12)$$

There are three real solutions when

$$\left(-\frac{1}{9} + \frac{1}{3}\frac{r}{p}\right)^3 + \left(-\frac{1}{27} - \frac{1}{3}\frac{r}{p} + \frac{1}{2}\frac{q}{p}\right)^2 < 0. \quad (13)$$

Otherwise, there is only one real solution, and we do not expect multiple equilibria in our model.

Figure 2 shows the parameter region where the simple model predicts three multiple equilibria. In this region, the solution corresponding to the smallest u is stable while the middle solution is unstable. Thus, model runs that start with initial conditions between the lowest and the middle solutions will equilibrate to the lower superrotating state. When the third solution (highest u) is a valid solution, we expect the system to go to this state if the initial conditions are above the middle solution. However, the solution with the highest u is generally not valid because $u > u_{0eq}$; in these cases, we expect that systems with initial conditions above the middle solution will equilibrate to a higher u steady state, for which we do not have a model. The stability of the different equilibria can be verified using a potential function (Moehlis, personal communication).

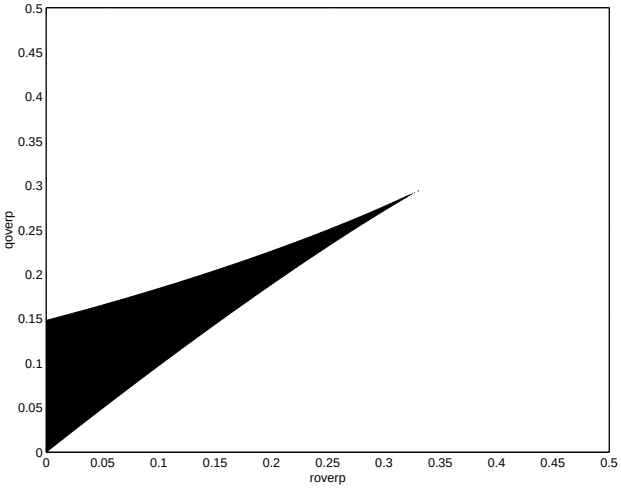

Figure 2: Region of multiple equilibria in analytical model. The dark region indicates values of $\frac{r}{p}$ and $\frac{q}{p}$ for which there exist multiple equilibria. q corresponds to the strength of the applied forcing; r corresponds to the friction; and p relates to the Hadley circulation.

We further examined the feedback in this simplified model. As the forcing increases, u increases, which in turn decreases the Hadley circulation. Thus, less mass is brought up from below to decelerate the upper layer. This deceleration can be thought of as a "damping" caused by the relaxation of the height to the equilibrium height.

We examine how u changes as the forcing changes:

$$\frac{\partial U}{\partial q} = \left(\frac{1}{p(U-1)^2 + r}\right)\frac{1}{1 + \frac{2U(U-1)}{(U-1)^2 + r/p}}.$$

When $\frac{\partial U}{\partial q}$ goes to infinity, U must jump to a different solution. This quantity goes to infinity when

$$U = \frac{2 \pm \sqrt{1 - \frac{3r}{p}}}{3}$$

The lower value corresponds the the maximum U of lower branch, while the upper value corresponds to minimum U of upper branch. (However, the upper branch is not well-modeled by the model because U is usually greater than 1.) When $\frac{r}{p} > \frac{1}{3}$, U never jumps to a different branch. When $r = 0$ (i.e. frictionless case) there is an abrupt transition at $U = \frac{1}{3}$.

We do not expect the computer model to match the analytic model exactly, because the computer model does not conserve angular momentum near the equator. The flux of momentum from the lower layer decreases the angular momentum in the computer model. However, the analytic model helps us understand the basic mechanisms of the full computer model.

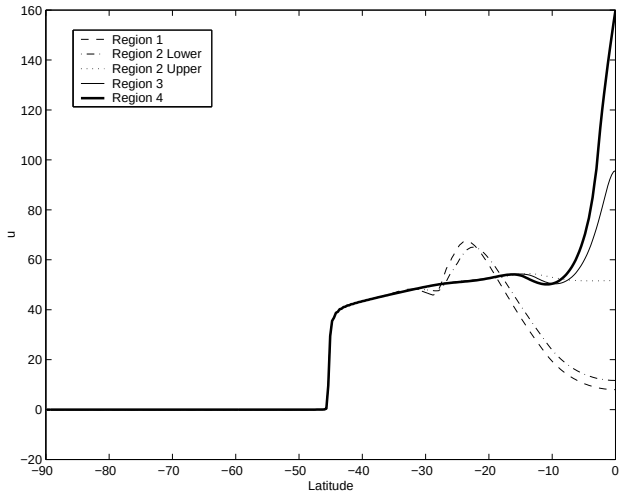

Figure 3: Steady state zonal velocity for $F_0 = 4 \times 10^{-7}$ (dashed), 5×10^{-7} lower branch (dash dot), 5×10^{-7} upper branch (dotted), 5.8×10^{-7} (thin), 8×10^{-7} (thick) for Run 2.

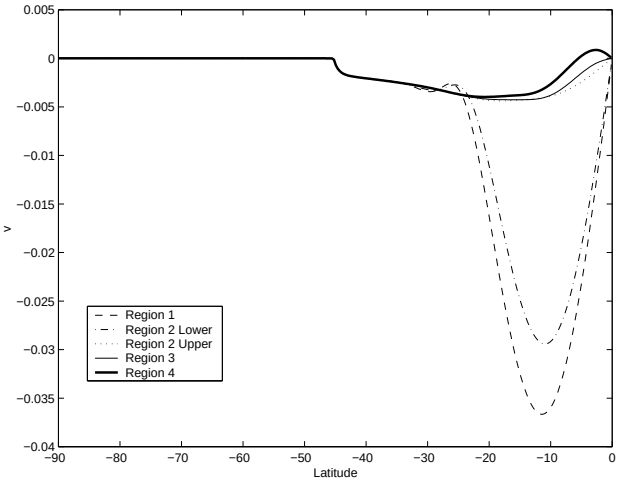

Figure 4: Steady state meridional velocity for $F_0 = 4 \times 10^{-7}$ (dashed), 5×10^{-7} lower branch (dash dot), 5×10^{-7} upper branch (dotted), 5.8×10^{-7} (thin), 8×10^{-7} (thick) for Run 2.

Run	Description	p	r	q
1	base run	0.051	0.0045	15000 $\times F_0$
2	narrower F ($n = 50$)	0.051	0.0045	15000 $\times F_0$
3	$k = 1 \times 10^{-8}$	0.051	0.009	15000 $\times F_0$
4	$g^* = 9.81 * 0.2$	0.0255	0.0045	15000 $\times F_0$

Table 1: Nondimensional parameters for each run.

4. RESULTS

We examined the stable steady states obtained by the full model by varying the forcing magnitude for different sets of parameters. In each run, there were four possible regions of different behavior depending on the magnitude of the forcing at the equator, F_0:

1. For small forcing, the system approximately agrees with the simple analytical model. The only stable solution is a Hadley-cell-like circulation with a small zonal velocity at the equator. The dashed lines in Figures 3 through 5 show an example of the steady solution in this region.
2. For slightly higher forcing, the system has two steady solutions. One approximates the expected Hadley cell circulation, while the other has a higher u and h. The dash-dot lines in Figures 3 through 5 show an example of the steady lower branch solution while the dotted lines show an example of the steady upper branch solution in this region.
3. When the forcing is further increased, the system has only one steady state. u is generally above u_{0eq}, but h is always below h_{eq}. The thin solid lines in Figures 3 through 5 show an example of the steady solution in this region.
4. For the highest values of the forcing, h_0 is above h_{0eq}. Thus the only term in the equatorial zonal momentum equation which can balance the forcing term is the friction term, and u_0 has only one possible value:

$$u_0 = \frac{F_0}{k}.$$

The thick solid lines in Figures 3 through 5 show an example of the steady solution in this region.

The size and location of the regions varied from run to run. The base run, Run 1, used the values given in section 2 and a wide forcing ($n = 30$). Table 1 describes how the other runs differed from Run 1 and lists nondimensional parameters for each run. Table 2 gives the ranges of the various regions.

The first two runs study the effect of the width of F on the full model. Figure 6 shows how U changes with the forcing in Run 2. Run 1 (not shown) looks similar. The location of the multiple steady equilibria region is within the range predicted by the simple analytical model. However, the range is always less than that predicted by the simple model. The region of multiple equilibria seems to be related to where the model closely conserves angular momentum in

Run	1	2	predicted 2	3	4
1	0-3.8	4.0-4.8	2.93-6.10	-	5.0-10
2	0-4.6	4.8-5.6	2.93-6.10	5.8-6	7-10
3	0-7.4	-	5.71-7.33	7.5-9.8	10.0-??
4	0-3.7	-	2.85-3.66	3.8-4.8	5.0-10.0

Table 2: Ranges of F_0 for the different solution regions. The values are in 10^{-7} ms^{-2}. A dash indicates that none of the tested values of F_0 corresponded to that region, though there may be untested values which do correspond to the region.

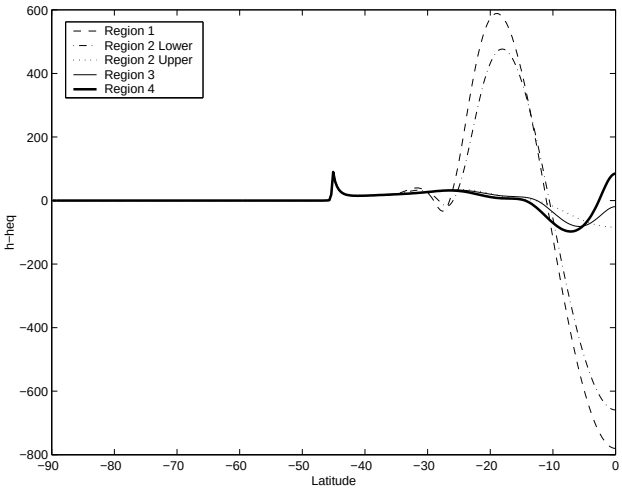

Figure 5: Steady state difference between layer height and relaxation height for $F_0 = 4 \times 10^{-7}$ (dashed), 5×10^{-7} lower branch (dash dot), 5×10^{-7} upper branch (dotted), 5.8×10^{-7} (thin), 8×10^{-7} (thick) for Run 2.

the tropics.

We found no steady state region in Run 3 (Figure 7) and Run 4 (not shown), though there are abrupt jumps in U near the predicted transition point from multiple to single equilibria), so there may be some very small region of multiple equilibria at this transition point.

5. CONCLUSIONS

It is possible to get bifurcations in the superrotation strength in an axisymmetric model for some parameter ranges. When bifurcations exist, the stable equilibria lie along two branches of U values as the forcing is changed. On the lower branch, damping due to height relaxation increases with increasing F_0; on the upper branch, the damping decreases with increasing F_0. Although the simple model approximately predicts where the full model will have multiple equilibria, the range is smaller than predicted and sometimes multiple equilibria are not present at all. The presence and location of the bifurcation has something to do with how well angular momentum is conserved in tropics, which depends on forcing. However, the exact relationship is not clear.

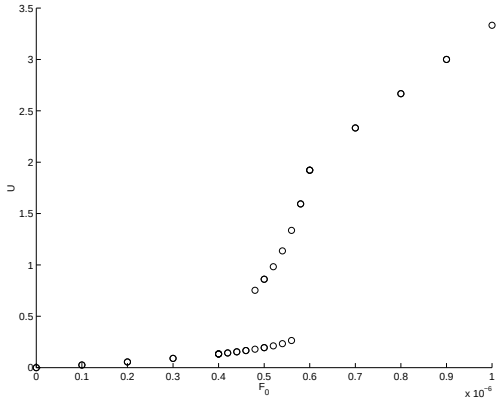

Figure 6: Nondimensional zonal wind at the equator for given values of the equatorial forcing for Run 2.

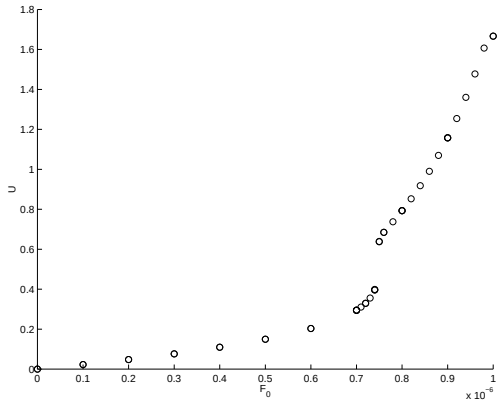

Figure 7: Nondimensional zonal wind at the equator for given values of the equatorial forcing for Run 3.

ACKNOWLEDGMENTS

This work was done primarily during the 2000 GFD Summer School. The authors would like to thank Jeff Moehlis for help with the nonlinear dynamics.

REFERENCES

Held, I. M., 2001: Equatorial superrotation in earth-like atmospheric models. *Bull. Am. Met. Soc.*, in preparation.

Held, I. M., A. Y. Hou, 1980: Nonlinear axially symmetric circulations in a nearly inviscid atmosphere. *J. Atmos. Sci.*, **37**, 515-533.

Huang, H.-P., and K. M. Weickmann, and C. J, Hsu: 2001: Trend in atmospheric angular momentum in a transient climate change simulation with greenhouse gas and aerosol forcing. *J. Clim.*, in press.

Saravanan, R., 1990: Ph.D. thesis, Princeton University, Princeton, NJ 08544.

Suarez, M. J. and D. G. Duffy, 1992: Terrestrial superrotation: A bifurcation of the general circulation. *J. Atmos. Sci.*, **49**, 1541-1554.